

a random effects model for segment travel times (see e.g., [1]), and consider trip travel time as an aggregated observation of segment travel times together with trip-level random effects. However, in practice, this is challenging because of the large dimensionality of the problem: to model the spatial correlation of segment travel time, two large covariance matrices, for inter-trip segment travel time and intra-trip segment travel time, respectively, need to be estimated from the aggregated travel time observations. For a transportation network with N segments, the covariance matrix is of size $N \times N$, which is computationally prohibitive for large networks. In addition, due to the sparse nature of GPS data, segment travel time for an individual trip often cannot be observed directly. Instead, the observed time interval between two consecutive GPS data points often reflects the aggregated travel time over multiple road segments. This also poses challenges in attributing the variation in total travel time on a path to each individual link on the path.

To effectively use GPS trajectories for learning trip travel time distributions, in this paper we propose the *ProbTTE* framework, which models the joint distribution of multiple trips as a multivariate Gaussian distribution. In particular, we design the covariance matrix to account for both inter-trip correlations and intra-trip correlations through learnable link/segment representations. In terms of training, we leverage the low-rank-plus-diagonal structure of the covariance matrix, and use negative log-likelihood as a loss function to update link representations. The link representation learned by *ProbTTE* also establishes a unified projection with a contraction property, which allows us to build efficient representations for trips through affine transformations of link representations. Additionally, a trip sub-sampling data augmentation method is developed to utilize the sparse GPS trajectories more efficiently for link representation learning. The main contributions of this paper are summarized as follows:

- We propose a multi-trip joint probabilistic distribution model *ProbTTE* for estimating travel times. Efficient low-rank parameterizations are introduced to learn inter-trip and intra-trip correlations among all segments in a transportation network.
- We propose a sub-sampling data augmentation approach to balance the samples and enhance the optimization efficiency in learning the link representation vectors. It facilitates specific optimization at the link level, enabling fine-grained modeling of link features.
- The experimental results on two real datasets validated the superiority of our model. Our model relatively outperforms the best deterministic and probabilistic baselines by an average of more than 12.11% and 13.34%, respectively. Ablation experiments and interpretability analysis further validate the effectiveness of multi-trip joint modeling and the learned link representation vectors.

The remainder of this paper is organized as follows. Section II summarizes related work. Section III introduces key definitions and formulations. Section IV presents the key components of *ProbTTE*, including parameterization of the inter-trip and intra-trip link covariance matrices and efficient

likelihood evaluation. We evaluate the proposed model on two real-world datasets in Section V. Finally, we conclude this study in Section VI.

II. RELATED WORK

In this section, we survey the work related to travel time estimation, covering both deterministic and probabilistic models, as the propaedeutics of our work. We summarize the comparison of the TTE-related work as shown in Table I.

A. Deterministic Travel Time Estimation

The methods for estimating travel time can mainly be divided into two categories based on the difference in input data. The first is based on Origin-Destination (OD) pairs [3]–[8]. Wang et al. [3] proposed a neighbor-based approach to find neighboring trips with exact origin/destination and simultaneously consider the dynamics of traffic conditions. They aggregate the travel time of neighboring trips to estimate the travel time of the query trip. To enrich the feature space of the input data, Li et al. [4] proposed a multi-task representation learning model for arrival time estimation (MURAT). It leverages more trip properties and the spatiotemporal prior knowledge of the underlying road network to produce trip representation based on a multi-task learning framework. Yuan et al. [5] introduced trajectory information to assist in matching neighboring trips during the training phase, but only OD information is utilized during the prediction phase. Road segment embeddings and time slot embeddings are utilized to represent the spatial and temporal properties of trajectories. Then, the hidden representation of OD input is trained to be close to the spatiotemporal representation of the trajectory. Similarly, Lin et al. [6] also utilized trajectory information during training. They partitioned the city into multiple pixels and utilized a Masked Vision Transformer to model the correlations between pixels. Then, they introduced a diffusion model for generatively encoding the OD and trajectory of the trip based on the spatiotemporal properties of pixels. In addition, Wang et al. [8] started considering constructing a probabilistic model within the OD-based method. They first infer the transition probability between road segments, then the most possible route can be recovered based on the given OD pair. The trip travel time can be obtained by calculating the sum of the travel times for all road segments on the recovered route. This method has broad applicability, low data requirements, and can be applied in scenarios where query trip trajectories are not available. However, the fuzzy nature of these input data makes it easy to lose key features of the trip, resulting in limited estimation performance.

The second method is route/path-based. In this approach, a trip is regarded as a sequence composed of links or GPS points. Deep neural networks are utilized to capture sequence features and generate estimations. Regarding GPS point data, Wang et al. [11] proposed embedding GPS points and their geographic information by incorporating geo-convolution and recurrent units to capture spatial and temporal dependencies. Liao et al. [10] propose a multi-faceted route representation learning framework that divides a route into three sequences:

TABLE I
COMPARISON OF TRAVEL TIME ESTIMATION MODELS.

Model Name	Model Type	Data Requirement	Probabilistic	Inter-trip Corr	Link Representation	Trip Representation
MURAT (2018) [4]	OD-based	OD Pair + Road Attributes			Graph Laplacian Regularization	OD Link Representation Concat
TEMP (2019) [3]	OD-based	OD Pair			—	OD Tuple
DeepOD (2020) [5]	OD-based	OD Pair + Road Attributes			Link and Attribute Embedding	OD Link Representation Concat
DOT (2023) [6]	OD-based	OD Pair			—	Masked Vision Transformer
MWSL-TTE (2023) [8]	OD-based	OD Pair + Road Attributes			Relational GCN	Direct Addition
DeepTTE (2018) [11]	Route-based	GPS Sequence + Trip Attributes			Geo-Conv	LSTM
WDR (2018) [15]	Route-based	GPS Sequence + Trip Attributes			Wide & Deep Model	LSTM
HetETA (2020) [16]	Route-based	GPS Sequence + Road Attributes			Het-ChebNet	Gated CNN
STTE (2021) [16]	Route-based	GPS Sequence + Road Attributes			Link and Attribute Embedding	LSTM
CatETA (2022) [13]	Route-based	GPS Sequence + Road Attributes + Trip Attributes			Link and Attribute Embedding	BiGRU
HierETA (2022) [21]	Route-based	GPS Sequence + Road Attributes			Link and Attribute Embedding	BiLSTM
MuT-TTE (2024) [21]	Route-based	GPS Sequence + Road Attributes			Link and Attribute Embedding	Transformer
DeepGTT (2019) [25]	Route-based	GPS Sequence + Road Attributes	✓		Link and Attribute Embedding	Link Representation Weighted Addition
RTAG (2023) [24]	Route-based	GPS Sequence + Road Attributes + Trip Attributes	✓		Link and Attribute Embedding	Self-attention
GMDNet (2023) [26]	Route-based	GPS Sequence + Road Attributes	✓		Link and Attribute Embedding	Self-attention with Position
ProTTE(ours)	Route-based	GPS Sequence	✓	✓	Link Embedding	Path-based-sum of Link Representation

GPS coordinates, the attribute of each road segment, and the IDs of road segments. Then, a transformer encoder is used to get the representations of three sequences. The authors fuse the multi-faceted route representations to get the estimation. Apart from directly processing GPS points, more studies involve first binding GPS points to the road network and then processing the link index. Wang et al. [10] formulated the problem of ETA as a pure regression problem and proposed a Wide-Deep-Recurrent (WDR) learning model to predict travel time along a given link sequence at a given departure time. It jointly trains wide linear models, deep neural networks, and recurrent neural networks together to take full advantage of all three models. Considering the potential additional time overhead at intersections between links, Han et al. [9] proposed a multi-semantic path representation method. It learns the semantic representations of link sequences and intersection sequences by considering information in non-Euclidean space and Euclidean space, respectively. Then a sequence learning component aggregates the information along the entire path and provides the final estimation. In addition, Hong et al. [16] propose HetETA to leverage heterogeneous information graphs in ETA tasks, translating the road map into a multi-relational network according to the connection direction at intersections between links. Temporal convolutions and graph convolutions are utilized to learn representations of spatiotemporal heterogeneous information. Considering travel time estimation as a classification problem is also a novel exploration. Ye et al. [13] proposed a Categorical approximate method to Estimate Time of Arrival (CatETA). It formulates the ETA problem as a classification problem and labels it with the average time of each category. Deep neural networks are designed to extract the spatiotemporal features of link sequences and obtain the estimation. These methods achieve excellent estimation performance through rich input features and mature sequence/graph neural networks. However, they only provide the mean travel time and cannot provide information on the fluctuation or confidence level of the prediction data.

B. Probabilistic Regression

Probabilistic regression, in contrast to deterministic regression, offers the advantage of providing uncertainty estimates alongside predictions, enhancing robustness and flexibility in modeling complex relationships. In economic analysis scenarios, probabilistic regression based on statistical methods has been widely researched. For example, ARCH, GARCH, etc. not only provide mean estimates but also model higher-order moments such as variance, offering a more comprehensive understanding of the data distribution. In recent years, the application of neural networks has provided new advancements in probabilistic regression. In [27], Salinas et al. proposed a recurrent neural network (RNN) architecture, named DeepAR, for probabilistic forecasting. It incorporates a negative binomial likelihood for count data as well as special treatment for the case where the magnitudes of the time series vary widely. Building upon this, the authors further propose a probabilistic high-dimensional multivariate forecasting method [28] to construct joint distributions for multivariate time series and measure the covariance between them. It parameterizes the output distribution based on a low-rank-plus-diagonal covariance matrix to reduce the number of parameters.

In TTE, there are also some efforts to explore probabilistic modeling. Li et al. [25] proposed a deep generative model to learn the travel time distribution by conditioning on the real-time traffic. This model interprets the generation of travel time using a three-layer hierarchical probabilistic model, which captures dynamically changing real-time traffic conditions and static spatial features, and then generates estimation times based on an attention mechanism. In [24], Zhou et al. proposed to learn the local representations of road segments over a temporal attributed graph, by jointly exploiting the dynamic traffic conditions and the topology of the road networks. Then a distribution loss based on the negative log-likelihood (NLL) is developed to fulfill the purpose of travel time distribution estimation. Mao et al. [26] introduced GMDNet, a Graph-based Mixture Density Network, which harnesses the advantages of both graph neural networks and mixture density networks for estimating travel time distribution. They utilized

the Expectation-Maximization (EM) framework to enhance stability during training. In addition, tensor-based methods have also been used to construct probabilistic estimation models for travel time.

These methods attempt to model the travel time of individual trips probabilistically. They assume that the travel times of trips are independent, overlooking the potential correlation among trips. This limits the feature perception range and impairs the estimation performance.

III. DEFINITIONS AND PROBLEM FORMULATION

A. Definition: Road Network

A road network is defined as the aggregate of all road segments within a studied area or a city. It is represented as a graph $\mathcal{G} = (\mathcal{V}, \mathcal{E})$, where \mathcal{V} denotes the set of nodes representing road segments/links, and \mathcal{E} denotes the set of edges illustrating the topological connections among these road segments. The terms ‘‘link’’ and ‘‘segment’’ are used interchangeably throughout this paper.

B. Definition: Links and Trips

A link $l \in \mathcal{V}$ refers to a road segment. Each link in the road network has a unique index. In this work, we follow OpenStreetMap (OSM) [29] to define links. The trajectory of a trip is an ordered sequence of time-stamped GPS records. For a trip with k GPS data points, we denote its trajectory by $T_q = \{(l_1, c_1), \dots, (l_k, c_k)\}$, where the time index c is monotonically increasing. The total travel time of the trip is $\tau = c_k - c_1$. Note that it is possible that (1) more than one GPS data points are located on the same link, and (2) a traversed link is not captured if no GPS records are registered. The link index sequence, after completing the entire sequence and removing duplicates, is used as model input, denoted by $T = \{l_1, \dots, l_k\}$. In other words, a trip T can be regarded as an ordered set of traveled links.

C. Problem Formulation

Given a dataset $\mathcal{D} = \{T_i | i = 1, \dots, N\}$ consisting of N historical trips in a road network, our objective is to estimate the probability distribution of the travel time τ_q for a query trip T_q that is not part of \mathcal{D} . In this paper, we consider the travel time τ_q to follow a Gaussian distribution:

$$\tau_q \sim \mathcal{N}(\mu_q, \sigma_q^2), \quad (1)$$

where $\mu_q = f_\mu(T_q)$ and $\sigma_q^2 = f_{\sigma^2}(T_q)$, and $f_\mu(\cdot)$ and $f_{\sigma^2}(\cdot)$ are two designed models for estimating the mean and the standard deviation of travel time τ_q , respectively.

IV. METHODOLOGY

A. Overview of *ProbtTE*

The overall architecture of *ProbtTE* is shown in Figure 1. A unique property of *ProbtTE* is that the correlation among multiple trips is explicitly modeled, and the travel times for multiple trips are jointly modeled as a multivariate Gaussian distribution. Each trip is represented by aggregating the low-rank representation of all those links that it covers. A neural

network-based mapping function is constructed to learn the mean travel time based on the trip representation vectors, while the covariance is formed using the inner product of these trip representation vectors for simultaneously modeling inter- and intra-trip correlations. Additionally, trip sub-sampling is used to augment the training data, balancing the samples and allowing gradients to differentially impact the representation at the link level within the same trip. Finally, historical trips in spatiotemporal proximity to the query trip are introduced to obtain the travel time distribution of a queried trip conditional on those observed trips. The final estimations are obtained by random sampling the conditional distribution. We explain the details of each component in the following subsections.

B. Parameterizing Link Travel Time Distribution

In this study, we focus on modeling trip travel time over a specific time horizon (e.g., 8:00–9:00 AM) of weekdays. In doing so, we restrict our scope to only model the variations in link travel time resulting from external factors rather than traffic demand. Given that the historical data spans several days, we employ a hierarchical model to describe both daily random fluctuations and random effects at the trip level. In particular, we model the travel time $t_{l,i,q}$ for link l , day i , and trip q as

$$t_{l,i,q} = \mu_l + \eta_{l,i} + \epsilon_{l,i,q}, \quad (2)$$

where μ_l represents the overall mean travel time for link l , which can be produced by link representation and other available covariates such as time of day and day of week, $\eta_{l,i}$ accounts for day-specific deviations as a result of the impacts of global unobserved factors that affects all trips in a day but are not used in modeling μ_l , such as weather conditions, road works and public holidays; and $\epsilon_{l,i,q}$ captures the trip-specific error (e.g., differences in driver/vehicle profile, or short-duration delays due to traffic incidents affecting multiple nearby links). This specification is similar to [1], where day-specific and trip-specific random effects are introduced to capture travel time variations.

For day-specific random effects, we assume the covariance $\text{Cov}(\eta_{l,i}, \eta_{l',i'}) = \delta(i, i') \times \Sigma_d(l, l')$, where $\delta(i, i') = 1$ when $i = i'$ and 0 otherwise, and Σ_d is a positive semi-definite matrix of size $|\mathcal{V}| \times |\mathcal{V}|$ characterizing inter-trip correlations. Thus, the joint distribution of travel times on all links on day i can be modeled as

$$\mathbf{x}_i = \boldsymbol{\mu} + \boldsymbol{\eta}_i \sim \mathcal{N}(\boldsymbol{\mu}, \Sigma_d), \quad (3)$$

where $\boldsymbol{\mu} \in \mathbb{R}^{|\mathcal{V}|}$ and $\boldsymbol{\eta}_i \in \mathbb{R}^{|\mathcal{V}|}$ are vectorized global mean and daily random effects, respectively. This specification also gives that \mathbf{x}_i and $\mathbf{x}_{i'}$ are independent if $i \neq i'$ (i.e., two different days).

Due to the large size of Σ_d , directly learning the Gaussian distribution in Eq. (3) will require a large number of parameters. For computational efficiency, we model Σ_d with a low-rank parameterization

$$\Sigma_d = LL^\top, \quad (4)$$

where $L \in \mathbb{R}^{|\mathcal{V}| \times r_L}$ and $r_L \ll |\mathcal{V}|$. With this assumption, Σ_d is positive semi-definite and we can consider each row of

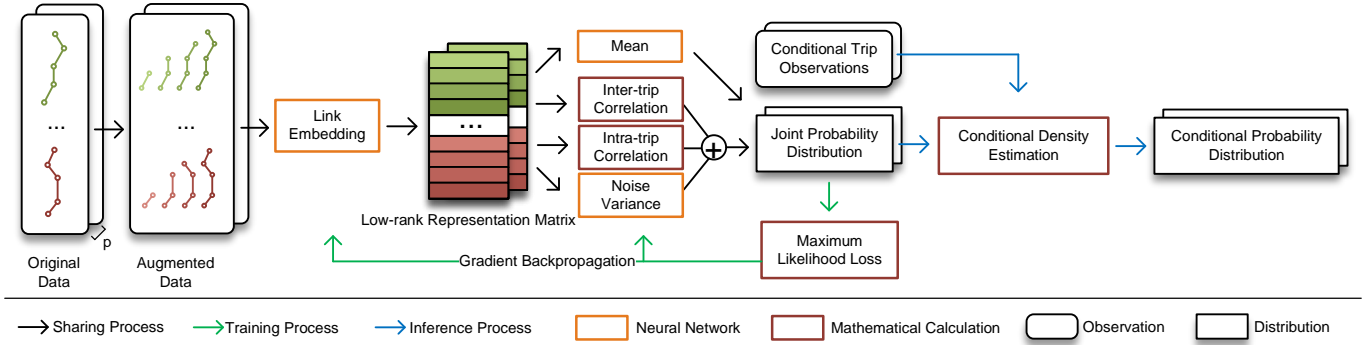


Fig. 1. Overall architecture of *ProbtTE*.

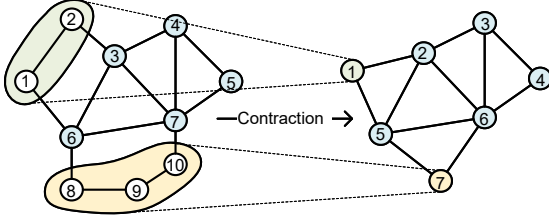


Fig. 2. Graph node contraction.

L as a representation vector of a link/segment. We adopt a multilayer perceptron $f_\mu(\cdot)$ to learn the global mean of travel time based on the representation matrix L

$$\boldsymbol{\mu} = L\mathbf{w}_\mu, \quad (5)$$

where $\mathbf{w}_\mu \in \mathbb{R}^{r_L}$ is a parameter vector to be learned. Combining Eqs. (5) and (4), we can specify the joint Gaussian distribution based on the link representation matrix L . It should be noted that the modeling of $\boldsymbol{\mu}$ is not limited to the segment feature L . One can also introduce other features that are available, such as driver/vehicle profile, time of day, day of week, public holiday information, and weather conditions. This will create a more comprehensive mean process. For example, Ref. [30] introduces representation learning for rare temporal conditions such as events and holidays.

In addition to computational efficiency, the proposed specification also provides excellent contraction properties and facilitates the aggregation of unimportant nodes in \mathcal{V} . For example, the contractions of links $\{1, 2\}$ and $\{8, 9, 10\}$ in Figure 2 can be achieved by introducing a 7×10 binary mapping matrix

$$M = \begin{bmatrix} 1 & 1 & & & & & & & & & \\ & & 1 & & & & & & & & \\ & & & \ddots & & & & & & & \\ & & & & 1 & & & & & & \\ & & & & & 1 & & & & & \\ & & & & & & 1 & & & & \\ & & & & & & & 1 & & & \\ & & & & & & & & 1 & & \\ & & & & & & & & & 1 & \\ & & & & & & & & & & 1 \end{bmatrix}. \quad (6)$$

Given the affine property of the Gaussian distribution, the mean travel time in the simplified network is $\boldsymbol{\mu}' = M\boldsymbol{\mu} = ML\mathbf{w}_\mu$ and the covariance matrix becomes $\Sigma'_d = ML(ML)^\top$. This corresponds to having a new representation matrix $L' = ML$. This affine property can further help us

in deriving the distribution of trip travel time. We define the representation of a trip (as a row vector) to be the path-based-sum of link representation vectors, i.e., ML , with $M \in \{0, 1\}^{1 \times |\mathcal{V}|}$. The mean travel time on a path becomes $M(L\mathbf{w}_\mu) = (ML)\mathbf{w}_\mu$ can be directly computed from the trip representation ML .

For the trip-level random effects $\epsilon_{l,i,q}$ in Eq. (2), we assume that it has a zero mean, i.e., $E(\epsilon_{l,i,q}) = 0$, and the covariance $\text{Cov}(\epsilon_{l,i,q}, \epsilon_{l',i',q'}) = \delta(i, i') \times \delta(q, q') \times \Sigma_p(l, l')$, where $\delta(q, q') = 1$ when $q = q'$ and 0 otherwise, and Σ_p is a $|\mathcal{V}| \times |\mathcal{V}|$ covariance matrix for modeling intra-trip error correlations. Note that we assume that trip-level random effects arise from driver/vehicle heterogeneity so that Σ_p is universal and shared for all trips. This assumption posits that the trip-level random effects are only correlated within the same trip and are independent between different trips.

For Σ_p , we propose a parameter-efficient low-rank-plus-diagonal parameterization to ensure that it is positive definite:

$$\Sigma_p = HH^\top + D, \quad (7)$$

where $H \in \mathbb{R}^{|\mathcal{V}| \times r_H}$ with $r_H \ll |\mathcal{V}|$ and $D \in \mathbb{R}^{|\mathcal{V}| \times |\mathcal{V}|}$ is diagonal matrix with $D_{i,i} > 0$ for $i = 1, \dots, |\mathcal{V}|$. In the neural network, we use a Softplus function nested with multilayer perceptron to model the diagonal entries $\text{diag}(D) = \log(1 + \exp(f_d(H)))$ where $f_d(H) = H\mathbf{w}_d$ and \mathbf{w}_d is a vector of length r_H . Similar to L , we can also perform contractions on the learned matrix H and the vector $\text{diag}(D)$.

C. Joint Distribution for Multiple Trips in a Day

A key challenge in learning the link representations is that trip-level link travel time $t_{l,i,q}$ is not observable in the raw GPS data. Instead, what we have is the final travel time for a trip. Let $\boldsymbol{\tau}_i = [\tau_i^1, \dots, \tau_i^{Q_i}]^\top \in \mathbb{R}^{Q_i}$ be the travel time observations for all trips on days i , where Q_i is the total number of trips on day i . We define a transformation matrix $A_i = [a_{q,l}] \in \{0, 1\}^{Q_i \times |\mathcal{V}|}$, where $a_{q,l} = 1$ if trip q uses link l and 0 otherwise, and denote the q -th row in A_i by A_i^q . We define $B_i = \text{blkdiag}(\{A_i^q\})$ of size $Q_i \times Q_i |\mathcal{V}|$ as a block diagonal matrix composed of each row in A_i . Marginalizing the day-specific and trip-specific random effects in Eq. (2), the joint distribution of $\boldsymbol{\tau}_i$ can be derived as

$$\boldsymbol{\tau}_i \sim \mathcal{N}(A_i\boldsymbol{\mu}, A_i\Sigma_d A_i^\top + B_i(I_{Q_i} \otimes \Sigma_p)B_i^\top), \quad (8)$$

where I_{Q_i} is an identity matrix of size Q_i and \otimes is the Kronecker product operator. As can be seen, the distribution in Eq. (8) implies that the travel times of two trips (q and q') on the same day are not independent, i.e., $\text{Cov}(\tau_i^q, \tau_i^{q'}) \neq 0$.

With the distribution in Eq. (8), we can learn the representation matrices (L and H) and the two parameter vectors (w_μ and w_d) by maximum likelihood. The total number of parameters is $|\mathcal{V}| \times (r_L + r_H + 2)$, and the parameters are shared for all trips on the road network. As mentioned, the parameters are designed for a specific time window of the day. Given the dynamic nature of traffic demand, time-varying link representation matrices $\{L^t, H^t\}$ are used to dynamically model the joint probability distribution. Here, we employ a simple method to discretize time for temporal modeling, with one day divided into several time intervals. Within each interval t , a separate set of embedding vectors $\{L^t, H^t, w_\mu^t, w_d^t\}$ is learned. We omit the time-interval index t for the rest of this paper.

The parameter $\theta = \{L, H, w_\mu, w_d\}$ of the model can be learned by maximizing the log-likelihood of all trip travel time observations. The log-likelihood of observing τ_i is

$$\mathcal{L}(\theta; \tau_i) \propto -\frac{1}{2} \left[\log \det(\tilde{\Sigma}) + (\tau_i - \tilde{\mu})^\top \tilde{\Sigma}^{-1} (\tau_i - \tilde{\mu}) \right], \quad (9)$$

where $\tilde{\mu} = A_i \mu$ and $\tilde{\Sigma} = A_i \Sigma_d A_i^\top + B_i (I_{Q_i} \otimes \Sigma_p) B_i^\top$. Calculating the log-likelihood requires computing the inverse and the determinant of $\tilde{\Sigma}$ of size $Q_i \times Q_i$, with time complexity of $\mathcal{O}(Q_i^3)$. In practice, the number of trips Q_i is often much larger than $|\mathcal{V}|$, and this becomes computationally infeasible. The issue can be potentially addressed by using a small batch size, which can still support the learning of all parameters. Nevertheless, this still requires the inversion of a matrix that matches the batch size, and employing a small batch size could result in inefficient training. In fact, we can effectively reduce the computational cost by leveraging the Woodbury matrix identity and the companion matrix determinant lemma:

$$\tilde{\Sigma}^{-1} = \Lambda^{-1} - \Lambda^{-1} V (I_{r_L} + V^\top \Lambda^{-1} V)^{-1} V^\top \Lambda^{-1}, \quad (10)$$

$$\det(\tilde{\Sigma}) = \det(I_{r_L} + V^\top \Lambda^{-1} V) \det(\Lambda), \quad (11)$$

where $\Lambda = B_i (I_{Q_i} \otimes \Sigma_p) B_i^\top$ is a diagonal matrix, $V = A_i L$ is a matrix of size $Q_i \times r_L$, and $V V^\top = A_i \Sigma_d A_i^\top$. With this procedure, the inverse $\tilde{\Sigma}^{-1}$ and its determinant can be calculated from $(I + V^\top \Lambda^{-1} V)$ of size $r_L \times r_L$.

D. Data Augmentation for Link Representation Learning

The joint distribution specified in Eq. (8) is designed for modeling overall trip travel time. This implies that only the initial and the final GPS data points are utilized, while the information in all the intermediate GPS data points is disregarded. Consequently, it becomes challenging to infer the distribution of day-level and trip-specific random effects, as they are only accessible through the aggregation by A_i . To address this issue, we propose a sub-sampling data augmentation approach of trips to effectively utilize the whole GPS trajectory of a trip. The original GPS sequence is subsampled to generate the sub-trips based on the observed GPS points. Particularly, considering the potential errors introduced by the

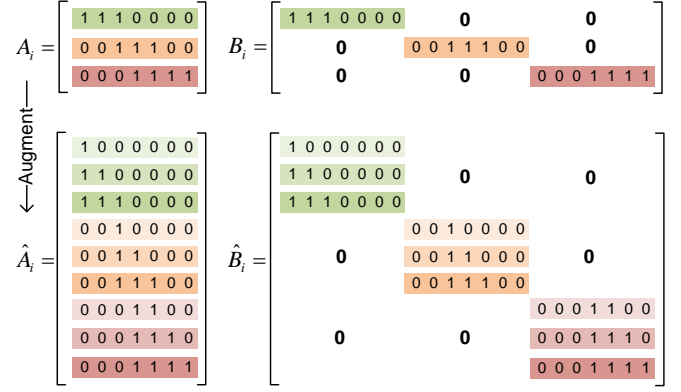


Fig. 3. Illustration for sub-sampling data augmentation.

limited GPS accuracy during the sub-sampling process, we only consider samples at the sub-trip granularity rather than at the link granularity. Excessively fine-grained sub-sampling may result in unreliable travel times for the samples.

We illustrate in Figure 3 a simple way of creating sub-trips. Here, we have 3 full trips that use 7 links. Directly following Eq. (8) will result in the unidentifiability issue. To make use of those intermediate GPS data points, for each trip we generate two subtrips by randomly selecting two intermediate GPS data points and consider them as the endpoints of the two subtrips. We treat the main trip and the two derived sub-trips as a set, and use this entire set to form a selection matrix \hat{A}_i^q from the vector A_i^q . The block diagonal matrix \hat{B}_i can also be constructed accordingly. Through this method, the augmented dataset now includes 9 trips due to the added intermediate GPS points, thus enhancing parameter learning. In this work, we sub-sample each original GPS trajectory T^0 of a trip into k new samples with a stride of rate $\eta \leq \frac{1}{k}$:

$$\begin{cases} T^1 = \text{Sub}(T, \eta) = \{l_1, \dots, l_{\eta|T|}\}, \\ \dots \\ T^k = \text{Sub}(T, \eta k) = \{l_1, \dots, l_{\eta k|T|}\}. \end{cases} \quad (12)$$

As can be seen, in this sub-sampling procedure, sub-trip T^k is created by selecting the first $\eta k|T|$ GPS points from the original trip, and we keep the trip start points to be the same for a set of trips. One can also use other approaches such as randomly selecting the startpoints and endpoints from available GPS data in creating sub-trips. For a mini-batch consisting of b full trips $\mathcal{T} = \{T_1^0, \dots, T_b^0\}$, we create k extra sub-trips $\{T_q^1, \dots, T_q^k\}$ for each trip T_q^0 following the aforementioned procedure. The augmented mini-batch can be represented by $\hat{\mathcal{T}} = \{\{T_1^0, \dots, T_1^k\}, \dots, \{T_b^0, \dots, T_b^k\}\}$, with $b(k+1)$ trips in total. The joint distribution of $\hat{\tau}_i = [\tau_1^0, \dots, \tau_1^k, \dots, \tau_b^0, \dots, \tau_b^k]^\top \in \mathbb{R}^{(k+1)b}$ becomes:

$$\hat{\tau}_i \sim \mathcal{N} \left(\hat{A}_i \mu, \hat{A}_i \Sigma_d \hat{A}_i^\top + \hat{B}_i (I_{Q_i} \otimes \Sigma_p) \hat{B}_i^\top \right), \quad (13)$$

where \hat{A}_i is composed by stacking $\{\hat{A}_i^q\}_{q=1}^b$ with $\hat{A}_i^q \in \{0, 1\}^{(k+1) \times |\mathcal{V}|}$ being the augmented selection matrix for trip q , and $\hat{B}_i = \text{blkdiag}(\{\hat{A}_i^q\})$. The distribution of the augmented trips (Eq. (13)) allows for more fine-grained gradient backpropagation in learning the representations for individual

links than the original distribution in Eq. (8).

In terms of computation, the likelihood can still be calculated following Eq. (9). However, when applying the Woodbury matrix identity and the matrix determinant lemma, we note that $\hat{\Lambda} = \hat{B}_i(I_{Q_i} \otimes \Sigma_p) \hat{B}_i^\top$ becomes a $b(k+1) \times b(k+1)$ block diagonal matrix, for which both the inverse and the determinant can be efficiently computed by working on each of the $(k+1) \times (k+1)$ blocks.

E. Conditional Travel Time Estimation based on Joint Probability Distribution

The joint distribution of trip travel times in Eq. (8) gives

$$\text{Cov}(\tau_i^q, \tau_i^{q'}) = A_i^q \Sigma_d A_i^{q'} = \sum_{l \in T_q} \sum_{l' \in T_{q'}} \Sigma_d(l, l'), \quad (14)$$

i.e., the covariance between two trips becomes the applying row-sum for $l \in T_q$ and then column-sum for $l' \in T_{q'}$ on the covariance matrix Σ_d . This indicates that any two trips in a given day are correlated, and the inter-trip correlation is determined by the values used in Σ_d . This result also means that we can make predictions for an unseen trip conditional on the correlated trips that are finished within the studied time window on the same day.

To estimate the travel time distribution of a queried trip, we can first explicitly estimate the distribution of η_i from those completed trips. Let $\begin{bmatrix} \eta \\ \tau_o \end{bmatrix}$ be a vector built by stacking the day-specific random effects η and (augmented) travel time τ_o of those completed trips on day i . Note that the day index i is omitted for simplicity. Then, we can derive its joint distribution as:

$$\begin{bmatrix} \eta \\ \tau_o \end{bmatrix} \sim \mathcal{N}\left(\begin{bmatrix} \mathbf{0} \\ A_o \mu \end{bmatrix}, \begin{bmatrix} \Sigma_d & \Sigma_d A_o^\top \\ A_o \Sigma_d & A_o \Sigma_d A_o^\top + B_o (I \otimes \Sigma_p) B_o^\top \end{bmatrix}\right) \quad (15)$$

and the conditional distribution $p(\eta \mid \tau_o = v)$ is also a Gaussian $\mathcal{N}(\mu^*, \Sigma^*)$, where

$$\begin{aligned} \mu^* &= \Sigma_d A_o^\top (A_o \Sigma_d A_o^\top + B_o (I \otimes \Sigma_p) B_o^\top)^{-1} (v - A_o \mu), \\ \Sigma^* &= \Sigma_d - \Sigma_d A_o^\top (A_o \Sigma_d A_o^\top + B_o (I \otimes \Sigma_p) B_o^\top)^{-1} \Sigma_d A_o. \end{aligned}$$

This conditional distribution can be also derived using precision matrix (i.e., the inverse of covariance), as $\eta \mid \tau_o = v \sim \mathcal{N}(\mu^*, (\Lambda^*)^{-1})$, where

$$\begin{aligned} \Lambda^* &= A_o^\top (B_o (I \otimes \Sigma_p) B_o^\top)^{-1} A_o + \Lambda_d, \\ \mu^* &= (\Lambda^*)^{-1} \left(A_o^\top (B_o (I \otimes \Sigma_p) B_o^\top)^{-1} (v - A_o \mu) \right), \end{aligned}$$

and $\Lambda_d = \Sigma_d^{-1}$.

This result is consistent with the estimator derived in [1]; however, our model explicitly learns the spatial structure of Σ_d and Σ_p using neural networks, instead of using oversimplified prior specifications. For the travel time τ of a queried trip with link incident matrix A , we can derive its distribution conditional on observed trip analytically:

$$\tau \mid \tau_o = v \sim \mathcal{N}(A(\mu + \mu^*), A(\Sigma^* + \Sigma_p)A^\top). \quad (16)$$

The conditional distribution obtained above, $p(\tau \mid \tau_o)$, can produce travel time statistics (mean/variance) of the query

Algorithm 1 *ProbTTE* Training Process

Input: batches of trips $\{T_1, \dots, T_b\}$

Output: travel time distribution $\tau \sim \mathcal{N}(\mu, \Sigma)$ of trips

- 1: Initialize link embedding network $E_Net1()$, $E_Net2()$
 - 2: Initialize multi-layer perceptrons $f_\mu()$, $f_d()$
 - 3: $L, H = E_Net1(l), E_Net2(l)$
 - 4: $A = \text{zeros}(b, |\mathcal{V}|)$
 - 5: $B = \text{zeros}(b, b \times |\mathcal{V}|)$
 - 6: **for** each T_i **do**
 - 7: **for** each $l \in T_i$ **do**
 - 8: $A_{i,l} = 1$
 - 9: $B_{i, \lfloor i/(k+1) \rfloor * |\mathcal{V}| + l} = 1$
 - 10: **end for**
 - 11: **end for**
 - 12: $\mu = f_\mu(AL) \in \mathbb{R}^{b \times 1}$
 - 13: $D = \log(1 + \exp(f_d(H))) \in \mathbb{R}^{b \times b}$
 - 14: $\Sigma = AL(AL)^\top + B(I_b \otimes (HH^\top + D))B^\top \in \mathbb{R}^{b \times b}$
 - 15: $\mathcal{L} = -\log \mathcal{N}(\hat{\tau} \mid \mu, \Sigma)$
 - 16: Backpropagation and update model parameters.
-

trips. For deterministic prediction, we can simply take the mean $A(\mu + \mu^*)$ as the point estimate. The training process is summarized in Algorithms 1.

V. EXPERIMENT

A. Datasets and Baselines

We evaluate *ProbTTE* on two publicly available GPS trajectory datasets from taxi/ride-hailing services: **Chengdu**: With 3,186 links and 346,074 samples spanning 6 days, travel times range from 420 to 2880 seconds, with a mean of 786 seconds; **Harbin**: With 8,497 links and 1,268,139 samples spanning 6 days, travel times range from 420 to 2994 seconds, with a mean of 912 seconds. The code and data are available at <https://github.com/ChenXu02/ProbTTE>.

We selected five state-of-the-art models as baselines, including three deterministic models and two probabilistic models.

Deterministic models:

- DeepTTE [11] is a model that learns spatial and temporal dependencies from raw GPS sequences through a geo-based convolutional layer and recurrent neural networks.
- HierETA [21] is a model that utilizes segment-view, link-view, and intersection representations to estimate the time of arrival. It captures local traffic conditions, shared trajectory attributes within links, and indirect factors, respectively, in a hierarchical manner.
- MulT-TTE [10] is a model that utilizes a multi-perspective route representation framework. It incorporates trajectory, attribute, and semantic sequences, together with a path-based module and self-supervised learning task, to enhance context awareness and improve segment representation quality for TTE.

Probabilistic models:

- DeepGTT [25] is a model that learns travel time distributions by incorporating spatial smoothness embeddings,

TABLE II
MODEL PERFORMANCE COMPARISON ON CHENGDU AND HARBIN DATASETS.

Model	Chengdu				Harbin			
	RMSE	MAE	MAPE(%)	CPRS	RMSE	MAE	MAPE(%)	CPRS
DeepTTE	181.31	130.10	17.20	—	224.23	162.59	18.36	—
HierETA	155.26	111.34	14.68	—	187.93	136.45	15.62	—
MuT-TTE	<u>149.77</u>	<u>105.63</u>	<u>13.89</u>	—	178.39	129.81	14.86	—
DeepGTT	165.17	118.68	15.65	1.46	191.23	143.97	16.41	1.56
GMDNet	151.43	107.73	13.97	<u>1.31</u>	<u>176.98</u>	<u>128.11</u>	<u>14.65</u>	<u>1.41</u>
<i>ProbTTE</i> [†]	134.79	95.11	12.31	1.18	156.94	112.15	12.82	1.24
<i>ProbTTE</i>	131.25	93.73	12.14	1.15	153.27	111.14	12.71	1.22
Improvement	12.37%	11.27%	12.60%	12.21%	13.40%	13.25%	13.24%	13.48%

amortization for road segment modeling, and a convolutional neural network for real-time traffic condition representation learning.

- GMDNet [26] is a model that estimates travel time distribution by employing a graph-cooperated route encoding layer to capture spatial correlations and a mixture density decoding layer for distribution estimation.

We also include a variant of our model, *ProbTTE*[†] in the comparison, which removes the conditional estimation component and is used to evaluate the naive predictive performance of our model when conditional information is unavailable.

We randomly select 70% of the dataset as the training set, 15% as the validation set, and 15% as the testing set. In terms of the model setting of *ProbTTE*, the batch size is $b = 64$, and the embedding dimension of the link representation vector $r_L = r_H = 36$. The time discretization coefficient $p = 24$. All models achieve optimal performance by training for 100 epochs on the 12th Gen Intel(R) Core(TM) i9-12900K CPU and NVIDIA Tesla V100 GPU. We choose four general evaluation metrics: Root Mean Square Error (RMSE), Mean Absolute Error (MAE), Mean Absolute Percent Error (MAPE), and Continuous Ranked Probability Scores (CRPS):

$$\text{RMSE} = \sqrt{\frac{1}{|\mathcal{D}|} \sum_{i \in \mathcal{D}} (\tilde{\tau}_i - \hat{\tau}_i)^2}, \quad (17)$$

$$\text{MAE} = \frac{1}{|\mathcal{D}|} \sum_{i \in \mathcal{D}} |\tilde{\tau}_i - \hat{\tau}_i|, \quad (18)$$

$$\text{MAPE} = \frac{1}{|\mathcal{D}|} \sum_{i \in \mathcal{D}} \left| \frac{\tilde{\tau}_i - \hat{\tau}_i}{\hat{\tau}_i} \right|, \quad (19)$$

$$\text{CRPS} = \frac{1}{|\mathcal{D}|} \sum_{i \in \mathcal{D}} \int (F(\tau_i) - 1_{\{\tau_i \geq \hat{\tau}_i\}})^2 d\tau_i, \quad (20)$$

where $F(\tau_i)$ is the cumulative distribution function of τ_i . $\tilde{\tau}_i$ is a randomly sampled value from the distribution of τ_i of query trip travel time and $\hat{\tau}_i$ is the ground truth.

B. Model Evaluation and Ablation Study

We summarize the experimental results in Table II. As can be seen, the proposed *ProbTTE* framework clearly outperforms all baseline models. In the Chengdu dataset, *ProbTTE* outperforms the deterministic baselines by over 1.75% in MAPE and

the probabilistic baselines by over 1.83% in MAPE and over 0.16 in CRPS. Compared to the best baseline, *ProbTTE* shows a relative average improvement of 12.11%. In the Harbin dataset, *ProbTTE* outperforms the deterministic baselines by over 2.15% in MAPE and the probabilistic baselines by over 1.94% in MAPE and over 0.19 in CRPS, respectively. Our model's performance has a relative average improvement of 13.34%. For the variant model *ProbTTE*[†], its performance in terms of MAPE is slightly lower than the full model *ProbTTE* by 0.17% and 0.11% on the Chengdu and Harbin datasets, respectively. However, it still maintains a significant advantage over the baseline models. This indicates that joint probability modeling across multiple trips can effectively learn correlations between trips, thus improving the accuracy of travel time estimation.

To further investigate the reasons for model superiority, we constructed three variants of *ProbTTE* focusing on Multi-trip Modeling, Data Augmentation, and Time Discretization:

- *ProbTTE*-w/o MT: The multi-trip modeling component is removed. Each batch contains only one trip, and the correlations between trips are not modeled.
- *ProbTTE*-w/o DA: The data augmentation component is removed. The trips are not subsampled, and only the original trip samples are used to train the model.
- *ProbTTE*-w/o TD: The time discretization component is removed. Only one set of parameters is used to learn the link embedding vector for all time periods.

We conducted ablation experiments on the Chengdu and Harbin datasets to analyze the effects of those components.

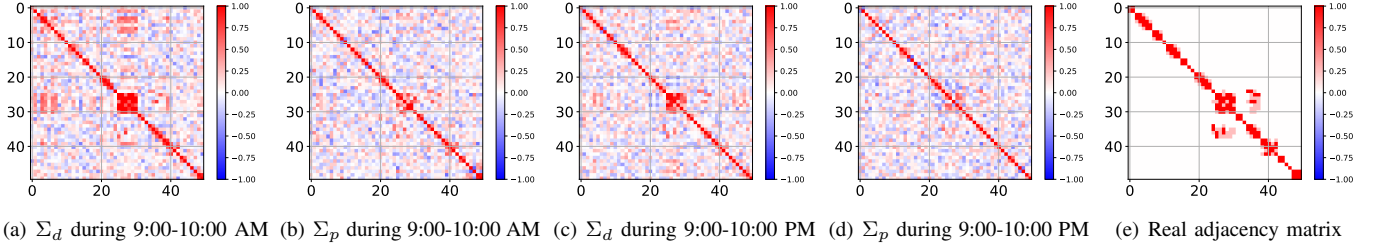
The results of the ablation experiments are shown in Table III. We can see that multi-trip joint modeling is the primary source of advantage for our model, contributing to a 2.11% and 2.59% improvement in reducing MAPE. The data augmentation based on subsampling has reduced MAPE by 0.52% and 0.44%, achieving performance improvement solely through reasonable segmentation of the original data without adding any model parameters. Time discretization resulted in gains of 0.48% and 0.32% for the model.

C. Interpretability Analysis of Link Embedding Vectors

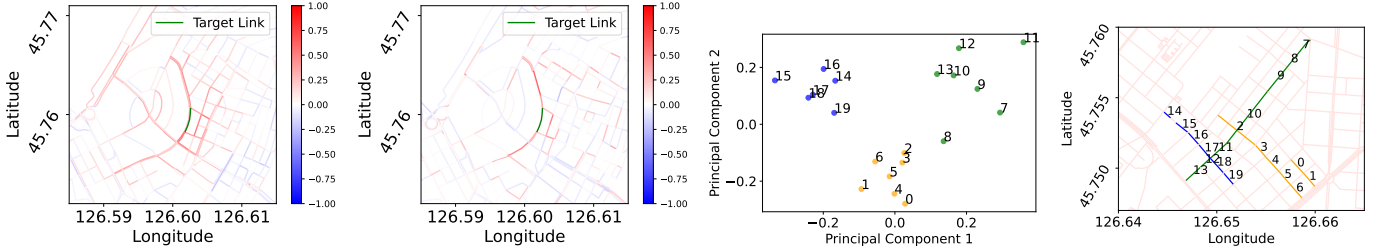
We analyze the interpretability of link embedding vectors and correlations on the Harbin dataset through data visualization. We visualized the learned link correlations Σ_d and Σ_p in two time periods (9:00-10:00 AM and 9:00-10:00

TABLE III
ABLATION EXPERIMENT ON CHENGDU/HARBIN DATASET.

Model	RMSE (s)	MAE (s)	MAPE (%)	CRPS
w/o MT	155.63/187.67	110.06/134.77	14.25/15.30	1.39/1.47
w/o DA	137.82/161.98	97.75/115.34	12.66/13.15	1.20/1.27
w/o TD	135.37/160.10	96.68/113.91	12.62/13.03	1.20/1.26
ProbTTE	131.25/153.27	93.73/111.14	12.14/12.71	1.15/1.23



(a) Σ_d during 9:00-10:00 AM (b) Σ_p during 9:00-10:00 AM (c) Σ_d during 9:00-10:00 PM (d) Σ_p during 9:00-10:00 PM (e) Real adjacency matrix



(f) Link correlation heatmap from Σ_d (g) Link correlation heatmap from Σ_p (h) Visualization of embedding vectors (i) Visualization of link locations

Fig. 4. Link correlation visualization.

PM), then compared them with the corresponding 2-hop real adjacency matrix, as shown in Figure 4(a,b,c,d,e). Despite not incorporating any network geometry information in the generation of link representations L and H , the derived link correlations still effectively capture the essential geometry information of the road network. Compared to the real adjacency matrix, the learned link correlations are more flexible and can adaptively construct correlations for different links. For example, some link correlations may have weak extensions, with high correlations lasting only 1 or 2 hops, while other links may exhibit stronger extensions, with high correlations persisting over multiple hops. In Σ_d , the learned correlations are smoother, reflecting global low-frequency characteristics, while in Σ_p , the learned correlations are sharper, representing high-frequency characteristics. Additionally, the correlation of links shows noticeable variations across different periods: it is stronger during peak hours and relatively weaker at night. In Figure 4(f,g), we randomly selected a link and visualized its correlations with other links in 9:00-10:00 AM on the real map and we can see that Σ_d indeed demonstrate long-range correlations, while the correlation structure in Σ_p is more local. Overall, the obtained Σ_d and Σ_p are consistent with our prior specification in Eq. (2), where Σ_d and Σ_p are used for modeling inter-trip correlation and intra-trip correlation, respectively. Next, we utilized Principal Component Analysis (PCA) to project the comprehensive representations of the link vectors $\{L, H\}$ into a two-dimensional space, and

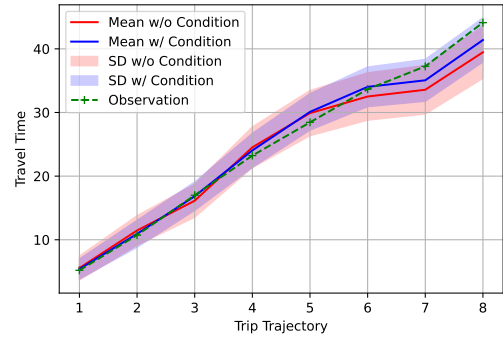


Fig. 5. Cumulative travel time (min) estimation: shaded area shows $\mu \pm \sigma$.

compared them with their actual map locations. As illustrated in Figure 4(h,i), vectors that are nearer in the representation space generally correspond to links that are closer on the map. Moreover, link representation vectors that run in the same direction on the same road tend to have higher similarity, whereas vectors from different roads show lower similarity. These results further confirm the effectiveness of $\{L, H\}$ as link representations.

We next visualize the mean and variance of travel times at the link level from one selected trip, which is divided into 8 segments with equal intervals of GPS points. Two scenarios are considered: with condition and without condition. In the conditional case, the travel times of 32 completed trips are

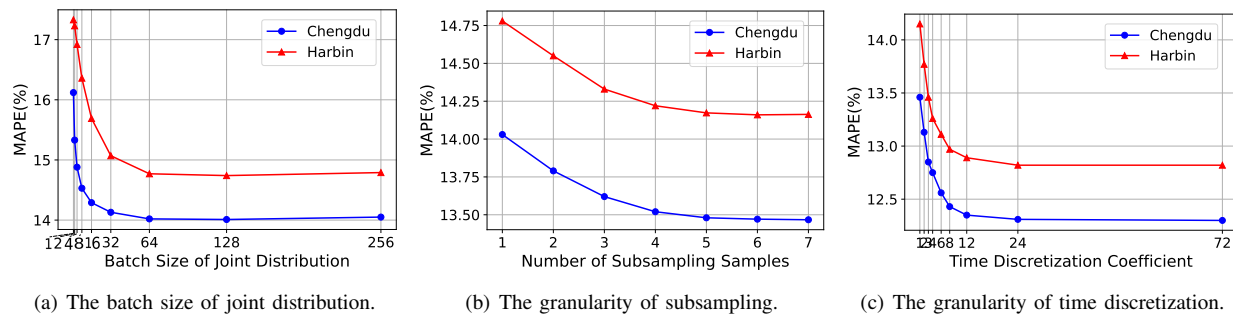


Fig. 6. Performance metrics associated with different configurations.

used as conditional information to adjust the distribution of the travel time for each link in the query trip. In the without-conditional case, only the learned link representation vectors are used to compute the mean and variance of the link travel times. The results, as shown in Figure 5, demonstrate that our model maintains good estimation performance and stability at the link level. The introduction of conditional information significantly reduces the prediction error and variance, and this positive adjustment becomes more apparent as the trip progresses.

D. Analysis of Model Parameters

1) *The batch size of the joint distribution:* We conducted a performance comparison of our model across various batch sizes of the joint distribution. To isolate the effects of other factors, we avoided introducing conditional trips, data augmentation, and time discretization. Therefore, our comparison solely reflects the performance achieved through multi-trip joint modeling using the original data. To enhance experimental efficiency, we adopted an exponential increase in the batch size, evaluating performance using $\{1, 2, 4, 8, 16, 32, 64, 128, 256\}$. As shown in Figure 6(a), the multi-trip joint modeling significantly improved prediction performance. When the batch size in the joint modeling increased, the MAPE saw a significant decline. However, upon reaching a specific threshold (approximately 32 trips), this decreasing trend slowed, and with additional increases in the number of trips, the MAPE started to increase marginally. We consider that multi-trip joint modeling offers additional information, allowing the model to identify relationships between trips. However, an excessively large batch size might strain the model’s optimization, making it more difficult to further improve performance and potentially leading to a performance plateau.

2) *The granularity of subsampling in data augmentation:* We analyzed the impact of data augmentation granularity on model performance. The original data was subsampled to generate $\{2, 3, 4, 5, 6, 7\}$ sub-trips, and the results are shown in Figure 6(b). In this evaluation, we followed the previous experiment and used 64 trips for joint modeling. As the granularity of data augmentation becomes finer, the model performance gradually improves. When the granularity is $\frac{1}{5}$ (number of subsampling samples is 5) the model performance reaches its optimum, and finer granularity does not lead to further improvement in performance.

3) *The granularity of time discretization:* We conducted a performance evaluation on temporal discretization based on the parameters determined in the preliminary experiments. We divided one day into $p = \{1, 2, 3, 4, 6, 8, 12, 24, 72\}$ periods and independently learned link embedding vectors for each period using separate parameters. As shown in Figure 6(c), the results indicate that the introduction of new trainable parameters improved the model performance. Fine-grained time discretization enables more accurate learning of link correlations, thereby enhancing model performance.

E. Analysis of Time Complexity

The time complexity of *ProbTTE* mainly comes from the mean and diagonal mapping, correlation computation, maximum likelihood estimation, and conditional distribution estimation. The time complexity of mean and diagonal mapping is $O(Nr)$. In correlation computation, the computational complexity is influenced by the number of trips in one joint probability distribution (batch size) b . N samples are divided into N/b batches, and the correlation of trips is calculated within each batch. The time complexity for calculating the inner product pairwise within each batch is $O(b^2r)$. So the total time complexity for correlation computation is $N/b * O(b^2r) = O(Nbr)$, where $r \ll N$. The final part of the computational complexity arises from maximum likelihood estimation and conditional distribution estimation. In these processes, with the help of the Woodbury Matrix Identity and the Matrix Determinant Lemma, the time complexity for inverting the covariance matrix and calculating the determinant is $O(rb^2)$, for N/b batches, the total time complexity is $O(Nbr)$. Therefore, the overall time complexity of *ProbTTE* is $O(Nr) + O(Nbr) + O(Nbr) = O(Nbr)$, where $b \ll N$, and $r \ll b$ in general.

We also conducted a comparison of the actual runtime of our model and the baselines. We recorded the time it took to train and infer one epoch for each model on the Chengdu and Harbin datasets. The device used for execution was an NVIDIA Tesla V100 GPU, and the runtime is shown in Table IV. The results indicate that our model achieves excellent performance without introducing excessive computational overhead.

VI. CONCLUSION

In this paper, we propose *ProbTTE*, a probabilistic TTE model designed to capture the joint probability distribution

TABLE IV
RUNTIME (S) OF MODELS.

Model	DeepTTE	HierETA	MuT-TTE	DeepGTT	GMDNet	<i>ProbtTE</i>
Chengdu	70.24	104.91	153.30	44.16	115.66	92.31
Harbin	199.67	349.50	491.45	158.91	425.37	315.64

of multiple trips. By introducing a covariance representation paradigm based on low-rank link representation, we effectively modeled correlations between trips with low time complexity and the learned representation gives favorable contraction properties. The use of subsampling data augmentation facilitated gradient propagation at the link level, resulting in the interpretable optimization of link representation vectors. *ProbtTE* demonstrated exceptional performance on real-world datasets, outperforming state-of-the-art deterministic and probabilistic baselines by 12.11% and 13.34% on average, respectively. Ablation experiments and visual analyses confirmed the effectiveness of each model component and the interpretability of the learned link representation vectors. Additionally, time complexity analysis and runtime comparisons illustrated that *ProbtTE* maintains a low computational burden while achieving superior performance in jointly modeling multiple trips.

In terms of future work, we plan to further explore the continuous modeling of link embedding vectors. Specifically, dynamic graph neural networks can be designed to learn low-rank temporal feature representations on a graph Laplacian basis from observed trips. Recurrent neural networks can subsequently be leveraged to capture the evolution of link embedding vectors based on the contextual information of observed trips. We believe that these enhancements will enable the model to better perceive temporal trends and facilitate the modeling of travel time distributions across multiple time horizons.

REFERENCES

- [1] C. Yan, J. Johndrow, D. Woodard, and Y. Sun, "Efficiency of eta prediction," *SIAM Journal on Mathematics of Data Science*, vol. 6, no. 2, pp. 227–253, 2024.
- [2] Y. Wang, Y. Zheng, and Y. Xue, "Travel time estimation of a path using sparse trajectories," in *Proceedings of the 20th ACM SIGKDD international conference on Knowledge discovery and data mining*, 2014, pp. 25–34.
- [3] H. Wang, X. Tang, Y.-H. Kuo, D. Kifer, and Z. Li, "A simple baseline for travel time estimation using large-scale trip data," *ACM Transactions on Intelligent Systems and Technology (TIST)*, vol. 10, no. 2, pp. 1–22, 2019.
- [4] Y. Li, K. Fu, Z. Wang, C. Shahabi, J. Ye, and Y. Liu, "Multi-task representation learning for travel time estimation," in *Proceedings of the 24th ACM SIGKDD international conference on knowledge discovery & data mining*, 2018, pp. 1695–1704.
- [5] H. Yuan, G. Li, Z. Bao, and L. Feng, "Effective travel time estimation: When historical trajectories over road networks matter," in *Proceedings of the 2020 ACM SIGMOD international conference on management of data*, 2020, pp. 2135–2149.
- [6] Y. Lin, H. Wan, J. Hu, S. Guo, B. Yang, Y. Lin, and C. S. Jensen, "Origin-destination travel time oracle for map-based services," *Proceedings of the ACM on Management of Data*, vol. 1, no. 3, pp. 1–27, 2023.
- [7] I. Jindal, X. Chen, M. Nokleby, J. Ye *et al.*, "A unified neural network approach for estimating travel time and distance for a taxi trip," *arXiv preprint arXiv:1710.04350*, 2017.
- [8] H. Wang, Z. Zhang, Z. Fan, J. Chen, L. Zhang, R. Shibasaki, and X. Song, "Multi-task weakly supervised learning for origin-destination travel time estimation," *IEEE Transactions on Knowledge and Data Engineering*, 2023.
- [9] L. Han, B. Du, J. Lin, L. Sun, X. Li, and Y. Peng, "Multi-semantic path representation learning for travel time estimation," *IEEE Transactions on Intelligent Transportation Systems*, vol. 23, no. 8, pp. 13 108–13 117, 2021.
- [10] T. Liao, L. Han, Y. Xu, T. Zhu, L. Sun, and B. Du, "Multi-faceted route representation learning for travel time estimation," *IEEE Transactions on Intelligent Transportation Systems*, 2024.
- [11] D. Wang, J. Zhang, W. Cao, J. Li, and Y. Zheng, "When will you arrive? estimating travel time based on deep neural networks," in *Proceedings of the AAAI conference on artificial intelligence*, vol. 32, no. 1, 2018.
- [12] Y. Sun, K. Fu, Z. Wang, D. Zhou, K. Wu, J. Ye, and C. Zhang, "Co-driver eta: Combine driver information in estimated time of arrival by driving style learning auxiliary task," *IEEE Transactions on Intelligent Transportation Systems*, vol. 23, no. 5, pp. 4037–4048, 2020.
- [13] Y. Ye, Y. Zhu, C. Markos, and J. James, "Cateta: A categorical approximate approach for estimating time of arrival," *IEEE Transactions on Intelligent Transportation Systems*, vol. 23, no. 12, pp. 24 389–24 400, 2022.
- [14] J. Qiu, L. Du, D. Zhang, S. Su, and Z. Tian, "Nei-tte: Intelligent traffic time estimation based on fine-grained time derivation of road segments for smart city," *IEEE Transactions on Industrial Informatics*, vol. 16, no. 4, pp. 2659–2666, 2019.
- [15] Z. Wang, K. Fu, and J. Ye, "Learning to estimate the travel time," in *Proceedings of the 24th ACM SIGKDD international conference on knowledge discovery & data mining*, 2018, pp. 858–866.
- [16] H. Hong, Y. Lin, X. Yang, Z. Li, K. Fu, Z. Wang, X. Qie, and J. Ye, "Heteta: Heterogeneous information network embedding for estimating time of arrival," in *Proceedings of the 26th ACM SIGKDD international conference on knowledge discovery & data mining*, 2020, pp. 2444–2454.
- [17] X. Fang, J. Huang, F. Wang, L. Zeng, H. Liang, and H. Wang, "Constat: Contextual spatial-temporal graph attention network for travel time estimation at baidu maps," in *Proceedings of the 26th ACM SIGKDD International Conference on Knowledge Discovery & Data Mining*, 2020, pp. 2697–2705.
- [18] Q. Wang, C. Xu, W. Zhang, and J. Li, "Graphtte: Travel time estimation based on attention-spatiotemporal graphs," *IEEE Signal Processing Letters*, vol. 28, pp. 239–243, 2021.
- [19] A. Derrow-Pinion, J. She, D. Wong, O. Lange, T. Hester, L. Perez, M. Nunkesser, S. Lee, X. Guo, B. Wiltshire *et al.*, "Eta prediction with graph neural networks in google maps," in *Proceedings of the 30th ACM international conference on information & knowledge management*, 2021, pp. 3767–3776.
- [20] G. Zou, Z. Lai, C. Ma, M. Tu, J. Fan, and Y. Li, "When will we arrive? a novel multi-task spatio-temporal attention network based on individual preference for estimating travel time," *IEEE Transactions on Intelligent Transportation Systems*, 2023.
- [21] Z. Chen, X. Xiao, Y.-J. Gong, J. Fang, N. Ma, H. Chai, and Z. Cao, "Interpreting trajectories from multiple views: A hierarchical self-attention network for estimating the time of arrival," in *Proceedings of the 28th ACM SIGKDD Conference on Knowledge Discovery and Data Mining*, 2022, pp. 2771–2779.
- [22] C. Wang, F. Zhao, H. Zhang, H. Luo, Y. Qin, and Y. Fang, "Fine-grained trajectory-based travel time estimation for multi-city scenarios based on deep meta-learning," *IEEE Transactions on Intelligent Transportation Systems*, vol. 23, no. 9, pp. 15 716–15 728, 2022.
- [23] X. Fang, J. Huang, F. Wang, L. Liu, Y. Sun, and H. Wang, "Ssm: Self-supervised meta-learner for en route travel time estimation at baidu maps," in *Proceedings of the 27th ACM SIGKDD Conference on Knowledge Discovery & Data Mining*, 2021, pp. 2840–2848.
- [24] W. Zhou, X. Xiao, Y.-J. Gong, J. Chen, J. Fang, N. Tan, N. Ma, Q. Li, C. Hua, S.-W. Jeon *et al.*, "Travel time distribution estimation

- by learning representations over temporal attributed graphs,” *IEEE Transactions on Intelligent Transportation Systems*, 2023.
- [25] X. Li, G. Cong, A. Sun, and Y. Cheng, “Learning travel time distributions with deep generative model,” in *The World Wide Web Conference*, 2019, pp. 1017–1027.
- [26] X. Mao, H. Wan, H. Wen, F. Wu, J. Zheng, Y. Qiang, S. Guo, L. Wu, H. Hu, and Y. Lin, “Gmdnet: A graph-based mixture density network for estimating packages’ multimodal travel time distribution,” in *Proceedings of the AAAI Conference on Artificial Intelligence*, vol. 37, no. 4, 2023, pp. 4561–4568.
- [27] D. Salinas, V. Flunkert, J. Gasthaus, and T. Januschowski, “Deepar: Probabilistic forecasting with autoregressive recurrent networks,” *International journal of forecasting*, vol. 36, no. 3, pp. 1181–1191, 2020.
- [28] D. Salinas, M. Bohlke-Schneider, L. Callot, R. Medico, and J. Gasthaus, “High-dimensional multivariate forecasting with low-rank gaussian copula processes,” *Advances in neural information processing systems*, vol. 32, 2019.
- [29] M. Haklay and P. Weber, “Openstreetmap: User-generated street maps,” *IEEE Pervasive computing*, vol. 7, no. 4, pp. 12–18, 2008.
- [30] N. Petersen, F. Rodrigues, and F. Pereira, “Representation learning of rare temporal conditions for travel time prediction,” in *2023 IEEE 26th International Conference on Intelligent Transportation Systems (ITSC)*. IEEE, 2023, pp. 4919–4926.